Vol. 04, Iss. 2 (2026) 235-255, DOI: 10.61552/JME.2026.02.009

JME

Journal of Materials and Engineering

www.jme.aspur.rs

Metal Halide Perovskites: Material Design, Fabrication Technologies, and Optoelectronic Applications

Safia[a], Waheed Ur Rehman[a,*], Amin Ur Rehman[a]

[a]*PCSIR, Laboratories Complex, Peshawar, Peshawar 25120, Pakistan*

Keywords:

Perovskites
Optoelectronics
Light-emitting diodes
Photodetectors

* Corresponding author:

Waheed Ur Rehman
E-mail: contactwaheed@hotmail.com

Received: 2 February 2026
Revised: 30 March 2026
Accepted: 11 May 2026

A B S T R A C T

In just over ten years, metal halide perovskites have gone from being a mineralogical curiosity to a cutting-edge material class, sparking a revolution in optoelectronics. Their remarkable mix of optoelectronic characteristics–long charge-carrier diffusion lengths, high absorption coefficients, and tunable bandgaps–as well as the possibility of low-cost, solution-based fabrication is what has propelled their explosive growth. As a result, solar cell power conversion efficiencies have increased from 3.8% to over 26%, and high-performance light-emitting diodes, photodetectors, and lasers are now possible. Two major obstacles stand in the way of commercialization, though: the environmental issues with lead-based compositions and operational instability in the presence of heat, light, and moisture. This review offers a thorough examination of the area relating applied technology to basic material features. It investigates the device's performance in various applications, synthesis techniques, and iconic crystal structure. Degradation mechanisms and methods to improve stability, including enhanced encapsulation, compositional engineering, and interface passivation, are given serious attention. Lastly, an evaluation of the advancements and challenges in creating lead-free substitutes is provided, providing a forward-looking view of the research required to produce sustainable and practical perovskite technologies.

1. INTRODUCTION

The historical account of perovskite materials includes geological discovery, serendipitous synthesis, and delayed recognition, culminating in a revolutionary technological paradigm. The expedition started in the Ural Mountains in 1839, when German mineralogist Gustav Rose found a calcium titanium oxide ($CaTiO_3$) mineral and named it "perovskite" after the Russian mineralogist Lev Aleksevich von Perovskite [1]. The name was only used in mineralogy for approximately a hundred years to refer to a group of oxides with the ABO_3 formula and a distinctive crystal structure. The modern perovskite era began with largely overlooked research on the synthesis of organic-inorganic hybrid compounds, particularly methylammonium lead trihalide ($CH_3NH_3PbX_3$, where X = Cl, Br, I), which highlighted their intriguing structural and electrical properties [2]. This work marked the preliminary advancement of the materials essential to the modern perovskite revolution, despite their potential being overlooked. The next important step was in the 1990s when Mitzi and her team at IBM made thin films of hybrid perovskites, with an emphasis on tin-based ones like $(C_4H_9NH_3)_2SnI_4$ [3]. They demonstrated their efficacy as semiconducting channels in field-effect transistors and underscored their exceptional luminous properties, so laying the foundation for solution-processable perovskite optoelectronics [4].

The most important thing was how it was used in photovoltaics. In 2009, Miyasaka's team, which was studying dye-sensitized solar cells (DSSCs), substituted the molecular dye with $CH_3NH_3PbBr_3$ and $CH_3NH_3PbI_3$ particles. This led to the first recorded perovskite-sensitized liquid-electrolyte solar cell [5]. Even though it was quite unstable, it had a power conversion efficiency (PCE) of 3.8% and a strong photovoltaic impact. The key event happened in 2012, when two things happened at the same time that made things more stable. Park and Grätzel replaced the liquid electrolyte with a solid-state hole transporter (spiro-OMeTAD), achieving an efficiency of 9.7% and enhanced stability [6]. Snaith's group also realized that perovskites were not only good at sensing but also good bulk semiconductors. They made a "meso-superstructured" solar cell with over 10% efficiency and showed amazing optoelectronic properties, like ambipolar charge transport [7].

This combination of stability and simple architecture sparked interest around the world. In 2013, PCE grew at an incredible rate that had never been witnessed before in the history of photovoltaics. The certified efficiencies for single-junction cells have increased from 3.8% to more than 26%, while the efficiencies for perovskite/silicon tandem cells have gone up to more than 33% [5, 8]. This remarkable advancement was sustained through ongoing innovation in compositional engineering–developing mixed-halide and mixed-cation (e.g., $FA^+/Cs^+/MA^+$) perovskites for enhanced stability and optimal bandgaps–alongside advanced crystal growth regulation and interface management [9, 10]. The demonstration of superior performance across various architectures, including flexible substrates and large-area modules, along with the extension into applications beyond photovoltaics–such as high-brightness light-emitting diodes (LEDs), lasers, and photodetectors–has established their position as a versatile, cost-effective platform for next-generation optoelectronics [11, 12]. The remarkable rise of perovskites is facilitated by a unique combination of exceptional optoelectronic properties–such as high absorption coefficients, tunable bandgaps, prolonged carrier diffusion lengths, and significant defect tolerance–coupled with the ability for low-temperature, solution-based fabrication [13, 14] . But there are a lot of big problems on the way to widespread commercialization. The main thing that keeps devices from lasting a long time is operational instability produced by stressors such moisture, oxygen, heat, and light, especially at device interfaces [15, 16]. The presence of toxic lead in high-performing compositions presents considerable environmental and health challenges, necessitating the development of efficient encapsulation techniques and lead-free substitutes [17, 18]. The transition from small-area champion cells to large-scale, stable, and reproducible modules presents a considerable engineering challenge, encompassing coating techniques, module interconnections, and manufacturing consistency [19]. This study is presented against a backdrop of great promise and pressing challenges. Our goal is to provide a comprehensive and analytical study of metal halide perovskites, linking basic research with practical technologies. We will analyze structure-property relationships, explore current advancements in synthesis and scalable fabrication, and do an extensive evaluation of performance in optoelectronic applications. A significant focus will be directed towards understanding degradation mechanisms and the strategic approaches–such as multidimensional structure, enhanced interface passivation, and resilient encapsulation–employed to augment operational stability [20, 21]. We will assess the progress in lead-free perovskites and other innovative material systems, providing a forward-looking appraisal of the research directions that are most likely to promote the commercial viability and sustainable incorporation of perovskite technology [22].

2. FUNDAMENTALS OF PEROVSKITE MATERIALS

2.1 Crystal Structure and Chemistry

The uncommon and flexible crystal structure of perovskite materials is what makes them so special. The word "perovskite" now generally refers to any material that has the crystal structure of calcium titanate ($CaTiO_3$), which is usually written as ABX_3. In this prototype framework, the cation at the A-site is usually large and has a single charge (for example, Cs^+ or $CH_3NH_3^+$ (MA^+)) and is in a 12-fold coordinated cuboctahedra configuration. The small B-site cation is divalent (for example, Pb^{2+} or Sn^{2+}) and sits in an octahedral site, where it is held in place by six anions. The X-site anion is usually a halide (like I^-, Br^-, or Cl^-) that connects the B-site cations. This makes corner-sharing $[BX_6]^{4-}$ octahedra that grow in a three-dimensional framework. The A-site cations fill in the empty spaces [1, 23]. This arrangement shows a lot of tolerance for changes at all points, which makes it easy to change the material's electrical, optical, and structural properties accurately. Goldschmidt's tolerance factor, *t*, and the octahedral factor, μ, show that this perovskite structure is stable and can be shaped. The tolerance factor, *t* = (r_A + r_X) / √2(r_B + r_X) (where *r* denotes the ionic radius), quantifies the geometric compatibility of ions; a *t* value ranging from approximately 0.8 to 1.0 is typically conducive to the formation of a cubic perovskite phase, with the optimal value nearing 0.9 [24, 25]. To ensure that the $[BX_6]$ octahedron is stable, the octahedral factor, μ = r_B / r_X, must be greater than about 0.41. Even though these requirements are based on observations, they are a necessary first step for predicting stable compositions and explaining phase transitions, as the change from tetragonal to cubic in $MAPbI_3$ when it is heated [26]. Recent advancements in machine learning techniques have improved these predictive models for discovering novel compositions [27].

The perovskite structure is strong because it may change its composition. You can change the functionality by adding different ions. Organic cations like methylammonium (MA^+) and formamidinium (FA^+) are common at the A-site. Inorganic cesium (Cs^+) is also used a lot to make things more thermally stable. Recent studies have demonstrated the efficacy of mixed A-site cations for enhanced performance and phase stability [28]. Lead (Pb^{2+}) is the most effective in the B-site, achieving the highest efficiencies. However, tin (Sn^{2+}) is the most researched lead-free alternative, despite the difficulties of oxidation (Sn^{2+} to Sn^{4+}) that are being addressed through advanced reducing agents and compositional regulation [29, 30]. At the X-site, iodide (I^-) produces the smallest bandgap for optimal light absorption, whereas bromide (Br^-) and chloride (Cl^-) increase the bandgap. Mixed-halide compositions (e.g., I/Br) enable continuous bandgap regulation, a critical attribute for tandem solar cells and light-emitting diodes (LEDs) [31]. Along with the 3D framework, dimensionality is also important in property engineering. Using larger ammonium cations that can't fit inside the cuboctahedral cavity makes it possible to break up the three-dimensional network into lower-dimensional shapes. Two-dimensional (2D) perovskites, such as the Ruddlesden-Popper (RP) and Dion-Jacobson (DJ) phases, have organic layers between inorganic slabs that create quantum and dielectric confinement. This makes them more stable and improves luminescence efficiency, but it also makes it harder for charges to move [32, 33]. Recent studies have focused on modifying the spacer cations in 2D perovskites to improve environmental stability while preserving charge transfer, making them very suitable for durable optoelectronic devices [34]. Further structural reduction leads to one-dimensional (1D) chain-like formations and zero-dimensional (0D) perovskites distinguished by isolated octahedra, primarily investigated for their strong, localized light emission and prospective application in high-color-purity white LEDs [35, 36]. This wide range of structures gives designers a lot of options for making materials with specific properties for certain uses.

2.2. Electronic and Optical Properties

The rapid emergence of metal halide perovskites is due to their astonishing optoelectronic capabilities, which are as good as or better than those of traditional semiconductors like silicon and gallium arsenide. The configurable bandgap is what makes this conceivable. Perovskites are different from many high-performance semiconductors that have fixed bandgaps because they have direct bandgaps that can be changed exactly over the visible and near-infrared spectrum (approximately 1.2 to 3.0 eV) by altering the composition. This is generally done by halide alloying (for example, combining I^- and Br^- in $MAPb(I_{1-x}Br_x)_3$) or by changing the A-site cation to change the tilt of the $[BX_6]^{4-}$ octahedra, which changes the valence and conduction band energies [31, 37]. Recent advancements have utilized this tunability to create complex multi-cation/halide compositions (e.g., mixed FA/Cs/K/Rb cations and I/Br anions) that achieve optimal bandgaps for tandem applications while simultaneously improving phase stability, driving certified perovskite/silicon tandem efficiencies beyond 33% [38, 39].

An exceptionally high absorption coefficient (>10^4 cm^{-1} near the band edge) is linked to the optimal bandgap. Perovskite thin films, which are only 300 to 500 nm thick, may be able to absorb most of the good sunlight. This is a significant advantage over conventional semiconductors like crystalline silicon, which need layers that are 100 to 200 times thicker to do the same thing [40]. This feature lowers the amount of materials used and the cost while improving the design of devices, making it possible to make efficient, ultra-thin, and portable optoelectronic devices. The creation of adaptive solar cells that work well and lightweight photodetectors based on perovskite has shown that they could potentially be used in wearable electronics and space applications [41, 42]. The narrow bandgap property makes them very good at collecting light because they can only absorb one photon at a time. Finding the phonon-assisted absorption process in lead-tin (Pb-Sn) mixed perovskites has helped us understand how bandgaps change and how low-bandgap (~1.2 eV) compositions absorb light, which is important for all-perovskite tandem cells [43, 44].

The most crucial distinctive electrical property of these materials is their outstanding charge carrier properties. Perovskites, on the other hand, show very long charge carrier diffusion lengths (over 1 μm in high-quality films) and high carrier mobilities [14, 45] even though they were processed from solution at low temperatures, which is usually associated with a lot of disorder and defects. Recent investigations of single crystals and optimized polycrystalline films have demonstrated that these characteristics can be further enhanced, with ambipolar diffusion lengths surpassing 10 μm and charge carrier lifetimes nearing 10 microseconds, metrics analogous to the highest-quality inorganic semiconductors produced via costly epitaxial techniques [46, 47]. This combination means that electrons and holes that are created by light can travel long distances without recombining. This is important for solar cells to work well and for lasers to accomplish population inversion. The phenomenon of "defect tolerance" is partially attributed to the low exciton binding energy, generally between a few meV and tens of meV, which facilitates the efficient generation of free charges from absorbed photons at room temperature, as opposed to bound electron-hole pairs (excitons) that require additional energy for dissociation [48]. We now have an extensive knowledge of where this fault tolerance comes from. This phenomenon grows from the distinctive electronic structure of lead-halide perovskites, which feature antibonding states at the valence band maximum and significant spin-orbit coupling. This results in a shallow defect potential and a decrease in deep-level trap states that typically facilitate non-radiative recombination [48, 49]. The outstanding functioning of perovskite optoelectronic devices is mainly owing to how easy it is to make them, how long it takes for them to recombine, and how easy it is to get free charges out of them. This is shown by the fact that charge carrier diffusion lengths are longer than the film thickness in commercially viable, blade-coated mini-modules. This means that better electrical quality may be kept during scaled production [50].

3. FOUNDATIONAL SYNTHESIS METHODOLOGIES AND FABRICATION TECHNIQUES

3.1 Solid-State Synthesis

This classical top-down approach remains the industrial backbone for producing bulk, polycrystalline perovskite oxides, relying on high-temperature inter-diffusion of solid precursors.

Standard Solid-State Reaction for Ceramics: This is the old-fashioned method that solid oxides react with each other. To create compounds like $Ln_{0.5}A_{0.5}FeO_{3-\delta}$, for example, high-purity oxides (such La_2O_3, Sm_2O_3, BaO, and Fe_2O_3) are mixed with a dispersant like 2-propanol in an agate mortar in the right amounts. The homogenized mixture is pelletized and calcined in air at 950°C for 2 h. The calcined material is subsequently ground, re-pelletized, and subjected to repeated calcination at progressively higher temperatures until a single-phase product is obtained, as shown in Table. 1 [51].

Synthesis with the Help of Mechanical Ball-Milling: Mechanical ball milling represents a significant advancement in the solid-state synthesis of multicomponent and doped oxide systems, where precise stoichiometric control is critical. The process involves a series of controlled physical transformations. In the synthesis of $Ca_{0.97-x}TiO_3$:Yb_3^{+}, Bi^{3+} phosphors, the starting materials are manually ground to achieve preliminary mixing at the macroscopic scale. This is followed by planetary ball milling using zirconia milling media in an alcohol medium for 4–12 hr. During this mechanochemical treatment, repeated fracturing and cold welding of particles occur, resulting in a substantial increase in surface area and the formation of fresh reactive interfaces. Subsequent high-temperature calcination (600–1500°C) provides the thermal energy required for solid-state ionic diffusion, promoting the formation and growth of a stable perovskite phase as shown in the Fig.1. Prolonged calcination times, extending up to 30 h, are often necessary to ensure complete reaction and to minimize point defects, mentioned in the Table.1. thereby enhancing functional properties such as luminescence [52].

Table 1. Comparative table of solid-state methodologies.

Technique Category	Specific Method	Key Principles/ Mechanism	Typical Temperature	Products/ Morphologies	Advantages	Critical Challenges /Limitations	Representative Materials
Solid-State Synthesis	Standard Solid-State Reaction [51]	High-temperature inter-diffusion of solid precursors; repeated grinding and calcination	950°C + progressive heating	Bulk polycrystalline ceramics, pellets	Industrial backbone, simple, scalable, no solvent requirements	High energy consumption, limited compositional control, large particle size, multiple heating steps	Ln0.5A0.5FeO3-δ, BaTiO3
Solid-State Synthesis	Mechanical Ball-Milling [52]	Mechanochemical treatment; repeated fracturing and cold welding; increased surface area for reaction	600–1500°C (calcination)	Fine powders, doped oxides	Enhanced kinetics, better stoichiometric control, reduced particle size	Extended milling times (4–12 h), prolonged calcination (up to 30 h), potential contamination from media	Ca0.97-xTiO3:Yb3+, Bi3+ phosphors

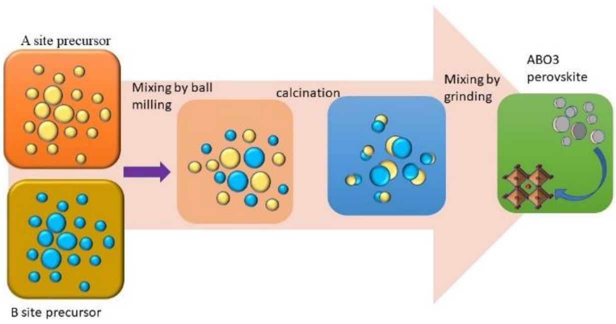

Fig. 1. Solid synthesis of perovskite material by Ball Milling.

3.2 Liquid-State (Solution) Synthesis

These bottom-up methods exploit molecular-level mixing in the liquid phase to exert unparalleled control over composition and morphology, operating at significantly lower temperatures than solid-state routes as compiled in Table 2.

Route for Glycine-Nitrate (Burning): This combustion synthesis, which can happen on its own, uses metal nitrates as oxidizers and glycine as fuel and a complexing agent. To make $Ln_{0.5}A_{0.5}FeO_{3-\delta}$ perovskites, metal nitrate solutions (such La_2O_3 dissolved in nitric acid or Ba $(NO_3)_2$) are mixed with glycine in a certain ratio of fuel to oxidizer (like 2:1 glycine/nitrate). When water evaporates, it turns into a thick gel that burns on its own at about 400°C, making a lot of powder. After that, the powder is made into pellets and burned at temperatures above 800°C to get rid of carbon residues and crystallize the pure phase [51].

Method of Freeze-Drying: This technique seeks to maintain cation homogeneity from the solution. A mixed nitrate solution for $Nd_{0.8}Sr_{0.2}(Mn_{1-x}Co_x)\ O_3$ is frozen drop by drop in liquid nitrogen and then sublimated under vacuum (freeze-drying). Slowly heating the amorphous precursor in air to about 600°C, breaks it down. Finally, heating the material repeatedly to 850°C in nitrogen (with grinding in between) makes the pure, crystalline perovskite phase [51].

Auto-Combustion: This method is a sophisticated example of solution combustion synthesis. The organic fuel (e.g., glycine, citric acid) acts as a complexing agent during the initial gel formation and later as a reducing agent in an exothermic redox reaction with metal nitrates (the oxidizer). The synthesis of $La_{0.7}Sr_{0.3}MnO_3$ exemplifies this: the mixture self-heats to 800–1000°C during auto-ignition, creating a transient "volcano" of heat that instantly crystallizes the oxide product while simultaneously generating a large volume of gases, which results in a highly porous, nanostructured foam. The subsequent calcination step is not for crystallization but for controlling the particle size and removing any residual carbonaceous material [53].

Sol-Gel Method: This is a cornerstone of soft chemistry, allowing for the fabrication of everything from ultra-fine powders to dense thin films. The process begins with **hydrolysis**, where metal alkoxides ($M(OR)_x$) react with water, replacing alkoxide groups with hydroxyls. This is followed by **condensation**, where these hydrolyzed species link via M-O-M bonds, releasing water or alcohol. The progressive extension of this network leads to **gelation**, forming a rigid, porous solid permeated by solvent. The **Pechini method**, a variant using chelating agents, is exceptionally powerful for multi-cation systems. The polymer network acts as a "molecular scaffold," immobilizing cations and preventing their segregation during the calcination step, which is crucial for achieving phase-pure materials like $La_{0.6}Ca_{0.4}MnO_3$ [54].

Co-Precipitation: The success of this method hinges on achieving a uniform supersaturation level for all cationic species simultaneously. For $LaMn_{1-x}Fe_xO_3$, the slow addition of a base (e.g., NaOH) to a mixed metal nitrate solution is performed under tightly controlled pH and stirring conditions to ensure the instantaneous and homogeneous nucleation of a mixed-metal hydroxide precursor. Any deviation can lead to sequential precipitation, resulting in compositional inhomogeneity. The washing step is critical to remove counter-ions (e.g., Na^+, NO_3^-), and the final calcination induces dehydration and crystallization into the desired perovskite oxide [53].

Table 2. Comparative table of liquid state methodologies.

Technique Category	Specific Method	Key Principles/ Mechanism	Typical Temperature	Products/ Morphologies	Advantages	Critical Challenges /Limitations	Representative Materials
Liquid-State Synthesis	Glycine-Nitrate Combustion [51]	Self-sustaining combustion; metal nitrates (oxidizer) + glycine (fuel/complexing agent); auto-ignition at ~400°C	~400°C (combustion); >800°C (post-annealing)	Fine, reactive powders	Rapid synthesis, low temperature initiation, good compositional homogeneity	Carbon residues require post-annealing, explosive reaction control needed	Ln0.5A0.5FeO3-δ
Liquid-State Synthesis	Freeze-Drying [51]	Dropwise freezing in liquid nitrogen; vacuum sublimation; maintains solution homogeneity	~600°C (decomposition); 850°C (crystallization)	Amorphous precursors → crystalline powders	Excellent cation homogeneity, preserves solution mixing state	Multiple heating steps, time-consuming sublimation process	Nd0.8Sr0.2(Mn1-xCox) O3
Liquid-State Synthesis	Auto-Combustion [53]	Complexation + exothermic redox reaction; transient "volcano" heating (800–1000°C)	800–1000°C (transient)	Nanostructured, highly porous foams	Instant crystallization, high porosity, large surface area	Rapid process difficult to control, carbon removal often needed	La0.7Sr0.3MnO3

Liquid-State Synthesis	Sol-Gel (incl. Pechini) [54]	Hydrolysis → condensation → gelation; polymer network as "molecular scaffold"	Low (gelation); variable (calcination)	Ultra-fine powders, thin films, aerogels	Molecular-level mixing, excellent compositional control, versatile end products	Shrinkage during drying, longer processing times, organic removal required	La0.6Ca0.4MnO3, multi-cation oxides
Liquid-State Synthesis	Co-Precipitation [53]	Simultaneous nucleation of all cations via pH control; homogeneous supersaturation	Ambient (precipitation); elevated (calcination)	Hydroxide precursors → oxide powders	Simple, rapid, good for large batches	Critical pH control, risk of sequential precipitation, washing essential	LaMn1₋xFexO3
Liquid-State Synthesis	Hydrothermal/ Solvothermal [55]	Pressurized autoclave; elevated T and autogenous pressure; increased precursor solubility	Below melting point (typically 150–250°C)	Nanocubes, nanowires, highly crystalline particles	Well-defined morphologies, low defect density, near-equilibrium growth	Pressure vessel required, limited batch size, longer growth times	SrTiO3, $BaTiO_3$ nanocrystals

Hydrothermal/Solvothermal Synthesis: This is a powerful technique for growing highly crystalline particles at temperatures significantly below their melting point. Precursors are dissolved or suspended in a solvent (water for hydrothermal, organic for solvothermal) and sealed in a pressurized autoclave. The elevated temperature and autogenous pressure increase the solubility and reactivity of the precursors, facilitating the crystallization of the perovskite phase. This method is renowned for producing well-defined morphologies like nanocubes and nanowires of materials like $SrTiO_3$ and $BaTiO_3$ with excellent control over particle size and low defect density, as the crystal growth occurs in a near-equilibrium condition [55].

3.3. Advanced Mechanochemical Synthesis

This signifies a paradigm change from thermally triggered to mechanically driven chemistry, facilitating novel reaction routes and phases.

High-Energy Ball-Milling (Mechanochemistry): High-speed milling (300–1000 rpm) can break chemical bonds, make metastable intermediates, and speed up kinetics by a huge amount. It works very well with hybrid perovskites. For instance, ball-milling MAI and PbI_2 without any solvents gives a quantifiable yield of $MAPbI_3$ in just a few minutes, overcoming solubility issues. The technique's strength is clear in how it keeps hard-to-find phases stable: Liquid-Assisted Grinding (LAG) using a small amount of solvent (like pentane) makes it easier for molecules to rearrange, which makes it possible to directly synthesize the photoactive α-$FAPbI_3$ at room temperature. This phase is normally stable, only above 150°C. Moreover, solid-state NMR verifies that mechanochemistry yields atomically homogenous mixed-halide perovskites (e.g., $MAPb(Br_xI_{1-x})_3$), devoid of the halide segregation regions that afflict solution-processed analogs [52].

3.4. Vapor-State Synthesis: Engineering Thin Films and Interfaces

These techniques are indispensable for depositing the high-purity, dense, and uniform thin films required for high-performance electronic and optoelectronic devices.

Chemical Vapor Deposition (CVD): This process involves a complex interplay of gas-phase and surface reactions. In Atmospheric Pressure CVD (APCVD), precursor vapors (e.g., PbI_2 and MAI) are transported by carrier gas to a heated substrate, where they adsorb, react, and form a solid film. The higher pressure leads to a boundary layer that can affect uniformity. Low-Pressure CVD (LPCVD) reduces this boundary layer, allowing for more conformal and uniform films, as demonstrated by the growth of large-grained $MAPbI_3$). The recent development of sequential CVD processes, where layers are deposited and reacted in steps, has enabled superior control over film morphology and crystallinity [56].

Hybrid Physical-CVD (HPCVD): This technique decouples the evaporation of precursors with different vapor pressures. Typically, a solid source like PbI_2 is thermally evaporated in high vacuum to form a uniform film. Subsequently, the organic halide (e.g., MAI) is sublimed in a controlled gas flow and diffuses to the substrate, where it reacts with the PbI_2 layer in a solid-vapor reaction. This method excels in producing exceptionally smooth, pinhole-free films with precise control over stoichiometry, making it a leading candidate for the fabrication of high-efficiency perovskite solar cells and their integration into perovskite-on-silicon tandem architectures [56].

Pulsed Laser Deposition (PLD): Pulsed laser deposition (PLD) is a flexible physical vapor method that is ideal for making high-quality oxide and halide perovskite films that fit perfectly without harming the layers below. PLD uses a solid target made by wet chemistry or solvent-free mechanochemical synthesis. This avoids problems with precursor solubility that come up with solution techniques. A major problem, though, is keeping the stoichiometry stable since organic and inorganic parts vaporize at different rates during ablation. To get stoichiometric transfer and the right film characteristics, researchers fine-tune important factors like deposition pressure, laser spot size, and substrate type. Because of this level of control, PLD is great for making complicated multilayer optoelectronic devices, like complete perovskite solar cells [57]. A comparative table is given below.

Table 3. Comparative table of vapor state methodologies.

Technique Category	Specific Method	Key Principles/ Mechanism	Typical Temperature	Products/ Morphologies	Advantages	Critical Challenges /Limitations	Representative Materials
Vapor-State Synthesis	Chemical Vapor Deposition (CVD) [56]	Gas-phase transport; adsorption; surface reaction	Variable (substrate heating)	Thin films, conformal coatings	High purity, uniform films, good for large areas	Complex precursor chemistry, vacuum equipment, boundary layer issues	MAPbI3 thin films
Vapor-State Synthesis	Low-Pressure CVD (LPCVD) [56]	Reduced pressure minimizes boundary layer	Variable	Highly uniform, conformal films	Superior uniformity vs APCVD, large-grained films	Vacuum equipment, slower deposition rates	Large-grained MAPbI3
Vapor-State Synthesis	Hybrid Physical-CVD (HPCVD) [56]	Sequential: thermal evaporation + solid-vapor reaction	Variable	Smooth, pinhole-free thin films	Exceptional smoothness, precise stoichiometry, ideal for tandem solar cells	Two-step process control, vacuum requirements	Perovskite solar cell layers
Vapor-State Synthesis	Pulsed Laser Deposition (PLD) [57]	Laser ablation of solid target; stoichiometric transfer	Variable	High-quality epitaxial thin films	Ideal for complex oxides, avoids solubility issues, multilayer capability	Stoichiometry challenges with mixed vapor pressures, line-of-sight deposition	Oxide and halide perovskites, complete solar cells

3.5 Synthesis of Nanocrystals and Low-Dimensional Structures

3.5.1 Colloidal Perovskite Nanocrystals (NCs)

The synthesis of perovskite NCs has unlocked a new realm of size- and shape-dependent properties, primarily for light emission.

Quantum Dots (QD): The **hot-injection method**, adapted from II-VI quantum dot synthesis, involves the rapid injection of a Cs-oleate precursor into a hot (140-200°C) solution of lead halide in a non-coordinating solvent. This creates a sudden supersaturation, leading to a short burst of nucleation followed by controlled growth, resulting in monodisperse $CsPbX_3$ NCs predicted in Table 4. Their spectacular optical properties—near-unity PLQY and narrow emission linewidths—stem from their defect-tolerant electronic structure and the effective passivation of surface traps by oleic acid and oleyl amine ligands [58].

The **Ligand-Assisted Reprecipitation (LARP):** This technique is a simpler alternative where a polar precursor solution is injected into a non-polar solvent, triggering instantaneous nucleation at room temperature mentioned in Table. 4 [59].

Nanowires (1D) & Nanoplates (2D): In Table 4. 1D and 2D Nanostructures creation were mentioned. The growth of 1D structures often proceeds through a solution-phase or vapor-phase oriented attachment mechanism, where initially formed nanocubes align and fuse along a specific crystal direction [60]. 2D nanoplatelets, such as $(BA)_2(MA)_{n-1}Pb_nBr_{3n+1}$, are typically synthesized using long-chain alkylammonium ligands (e.g., butylammonium, BA) that act as structure-directing agents. Their large steric bulk limits crystal growth in one dimension, resulting in quantum-confined sheets whose thickness (the value of 'n') and thus optical properties can be precisely controlled [61].

3.5.2 Single-Crystal Growth

Polycrystalline thin films are plagued by grain boundaries that act as recombination centers and ion migration pathways. Single crystals provide a defect-scarce platform to measure the fundamental limits of perovskite performance.

Inverse Temperature Crystallization (ITC): The ITC method for making $MASnI_3$ films uses a saturated precursor solution of MAI and SnI_2 in a 7:3 GBL: DMSO solvent mix. The filtered solution is in a sealed vial with a substrate. It is heated slowly from 50°C to 80–100°C at a rate of 1–2°C per hour. This takes use of retrograde solubility, which means that solubility decreases as temperature rises. This makes it possible to control nucleation and lateral expansion of a continuous single-crystal layer on the substrate. The process takes place in a sealed environment to keep Sn^{2+} from oxidizing. After that, the film is cooled, washed with toluene, and dried [62].

Bridgman-Stockbarger Method: This is a classic melt growth technique for high-quality, large-volume single crystals. The precursor powder is sealed in an ampoule, melted in a hot zone, and then slowly translated through a steep temperature gradient into a cold zone. The slow cooling at the solid-liquid interface ensures a single nucleation event and the progressive growth of a large, high-purity single crystal. This method is particularly suited for halide perovskites like $CsPbBr_3$ that melt congruently without decomposition [63].

Table 4. Comparative table of nano crystals methodologies.

Technique Category	Specific Method	Key Principles/ Mechanism	Typical Temperature	Products/ Morphologies	Advantages	Critical Challenges /Limitations	Representative Materials
Nanocrystal Synthesis	Hot-Injection [58]	Rapid injection into hot solvent; burst nucleation → controlled growth	140–200°C	Monodisperse quantum dots	Near-unity PLQY, narrow emission, defect-tolerant	Air-sensitive, batch-to-batch variability, ligand management	CsPbX3 (X = Cl, Br, I) quantum dots
Nanocrystal Synthesis	Ligand-Assisted Reprecipitation (LARP) [59]	Polar → non-polar solvent injection; instantaneous nucleation	Room temperature	Nanocrystals	Simple, room temperature, rapid	Less monodisperse than hot-injection	Perovskite nanocrystals
Nanocrystal Synthesis	Oriented Attachment/Structure-Directing [60, 61]	Alignment and fusion of nanocubes; long-chain ligands as structure directors	Variable	Nanowires (1D), nanoplatelets (2D)	Controlled dimensionality, quantum-confined properties	Precise ligand control required	(BA)2(MA)n-1PbnBr3n+1 nanoplatelets
Single-Crystal Growth	Inverse Temperature Crystallization (ITC) [62]	Retrograde solubility; slow heating induces controlled nucleation	50→80–100°C	Single-crystal films on substrates	Defect-scarce, measures fundamental limits, reduced grain boundaries	Narrow temperature window, oxidation-sensitive materials require sealing	$MASnI_3$ films
Single-Crystal Growth	Bridgman-Stockbarger [63]	Melt growth; slow translation through temperature gradient	Above melting point	Large-volume bulk single crystals	High purity, large crystals, classic melt technique	Requires congruent melting, thermal stress, ampoule sealing	CsPbBr3 bulk crystals

4. ADVANCED FABRICATION TECHNIQUES FOR FUNCTIONAL DEVICES

4.1 Thin-Film Deposition for Optoelectronics

The transition from a chemical precursor to a functional thin film is the most critically determining step in device fabrication mentioned in the Table 5.

Spin-Coating and Anti-Solvent Quenching: The anti-solvent method is a common way to make high-quality $MAPbI_3$ perovskite films. It starts with a solution of MAI and PbI_2 in solvents like DMF/DMSO. In spin-coating, an anti-solvent (like toluene) is put on the spinning substrate to quickly cause local supersaturation. This starts quick heterogeneous nucleation and solidifies the parts into a uniform intermediate complex (like MAI-PbI_2-DMSO). After that, heat annealing turns the intermediate phase into a crystalline layer. The method depends a lot on precise timing, solvent miscibility, and boiling points. This is because the anti-solvent must not mix with perovskite but must mix with the precursor solvents in order to get rid of residuals and make crystallization easier to control. The quick kinetics could cause morphological problems like pinholes and irregular grains. This makes the dripping window and volume ratio very important for reproducibility. Even with this problem, effective anti-solvent treatment is necessary to provide uniform films for photovoltaics and other optoelectronic uses [64].

Scalable Coating Techniques: For commercialization, methods like blade coating and slot-die coating are essential. These are meniscus-guided coating techniques where the ink is physically spread across the substrate. The challenge lies in formulating inks with a wide "processing window" the range of coating speeds, temperatures, and ambient conditions that still yield high-quality films. Recent research focuses on solvent engineering and additive strategies to control crystallization kinetics during the fast drying conditions of these scalable methods [65].

Vacuum Deposition: The FAMAPI film was made by co-evaporating PbI2, MAI, and FAI. Each of the three precursors was heated in its own thermally controlled crucible, which was separated from the others by thermal barriers. When the organic ammonium salts are first heated, they release gas, which causes the pressure in the chamber to rise temporarily. After that, the pressure quickly returns to normal. We used special quartz crystal microbalance (QCM) sensors placed near the PbI2 and FAI sources to measure how quickly they evaporated. We made sure that the temperatures stayed the same throughout the process. A QCM sensor placed close to the substrate holder controlled the evaporation of MAI. The QCM sensor was exposed to the flows of PbI_2, FAI, and MAI all at once. The best net evaporation rate was kept by changing the temperature of the MAI source during the evaporation process [66].

4.2 Freestanding Single-Crystal Membranes:

The ability to create freestanding, single-crystal oxide membranes allow for the integration of functional perovskites with arbitrary substrates, such as silicon photonics chips or flexible polymers, opening new avenues for "oxide electronics."

Sacrificial Layer Etching: This is how surface release works. The first step is to epitaxially deposit a water-soluble layer, usually $Sr_3Al_2O_6$ (SAO), on a suitable substrate, like $SrTiO_3$. After that, the chosen perovskite layer (such $SrRuO_3$ or $BaTiO_3$) is deposited on top of SAO in an epidermal way. The entire stack is put in water, which gets into and breaks down the SAO layer. This "frees" the top perovskite film as a separate membrane. To avoid breaking and reduce strain, the sacrificial layer and the functional film must be compatible with each other's lattices. Improved versions of this procedure use different sacrificial layers (such LSMO etched with HCl) that are made for specific material systems. How etching a sacrificial layer changes the properties of perovskite membranes [67].

Remote Epitaxy on Graphene: This groundbreaking technique leverages the unique electronic transparency of graphene. A single layer of graphene is transferred onto an epi-ready substrate (e.g., GaAs or $SrTiO_3$). During vapor-phase deposition, the potential field of the crystalline substrate "peeks through" the atomically thin graphene, templating the epitaxial growth of the perovskite film. However, the physical adhesion to the graphene is weak, allowing the subsequent mechanical peeling of a single-crystal membrane, while the original substrate, protected by graphene, can be reused indefinitely [68].

4.3 Additive Manufacturing and Patterning

For the integration of perovskites into complex device architectures, precise patterning is required.

Inkjet Printing: This digital, non-contact method deposits perovskite ink in the form of microscopic droplets onto a substrate, allowing for direct, maskless patterning of pixels for display applications or custom-shaped solar cells. The success of this method relies heavily on ink formulation, requiring optimal viscosity, surface tension, and colloidal stability to prevent clogging and ensure uniform droplet formation [69].

Nanoimprint Lithography: This technique involves pressing a patterned stamp into a soft, precursor-containing polymer film. After the stamp is removed, a relief pattern is left behind, which is then converted into a perovskite pattern via thermal annealing. This allows for the direct, high-throughput patterning of perovskite nanostructures with feature sizes down to a few tens of nanometers for nanophotonic and laser applications [70].

Table 5. Comparative table of Advanced fabrication methodologies.

Technique Category	Specific Method	Key Principles/ Mechanism	Typical Temperature	Products/ Morphologies	Advantages	Critical Challenges /Limitations	Representative Materials
Advanced Thin-Film Fabrication	Spin-Coating + Anti-Solvent Quenching [64]	Rapid supersaturation via anti-solvent; intermediate complex formation → annealing	Ambient (coating); elevated (annealing)	Uniform polycrystalline thin films	Industry standard for lab-scale, high-quality films, simple equipment	Critical timing, solvent miscibility issues, reproducibility challenges, pinhole risk	$MAPbI_3$ photovoltaic films
Advanced Thin-Film Fabrication	Blade Coating / Slot-Die Coating [65]	Meniscus-guided; physical ink spreading	Ambient to moderate	Large-area thin films	Scalable, compatible with roll-to-roll, commercial potential	Wide processing window required, crystallization control during fast drying	Perovskite solar cells (large-area)
Advanced Thin-Film Fabrication	Vacuum Co-evaporation [66]	Multiple thermally controlled sources; QCM monitoring	Variable	Thin films with precise composition	Excellent thickness control, no solvent issues, high purity	Complex equipment, rate monitoring challenges, organic salt degassing	FAMAPI films (PbI2 + MAI + FAI)
Freestanding Membranes	Sacrificial Layer Etching [67]	Epitaxial growth on water-soluble layer (e.g., Sr3Al2O6); selective etching	Epitaxial growth T; ambient etching	Freestanding single-crystal membranes	Integration with arbitrary substrates (Si, polymers), enables "oxide electronics"	Lattice matching required, strain management, delicate handling	SrRuO3, BaTiO3 membranes
Freestanding Membranes	Remote Epitaxy on Graphene [68]	Graphene as "transparent" template; substrate potential fields guide growth	Vapor deposition T	Peelable single-crystal membranes	Substrate reusable, mechanical peeling, avoids etching damage	Graphene transfer quality, weak adhesion control, epitaxial registry	Perovskites on GaAs or SrTiO3 substrates
Additive Manufacturing	Inkjet Printing [69]	Digital droplet deposition; maskless patterning	Ambient to moderate	Patterned films, pixels, custom shapes	Direct patterning, material efficiency, digital control	Ink formulation critical (viscosity, stability), nozzle clogging	Display pixels, custom solar cells
Additive Manufacturing	Nanoimprint Lithography [70]	Patterned stamp → soft film → annealing	Ambient (imprint); elevated (annealing)	Nanostructures with <100 nm features	High-throughput, sub-10 nm resolution, direct patterning	Stamp fabrication, pattern fidelity during conversion	Nanophotonic and laser structures

5. APPLICATIONS OF PEROVSKITE MATERIALS

Metal halide perovskites have amazing optoelectronic properties, such as an adjustable bandgap, a high absorption coefficient, strong luminescence, and excellent charge transport. Such features have made it easy for them to be used in several technologies. Photovoltaics is the most advanced field, but researchers are working hard to find new uses for them in light emission, detection, and other areas interpreted in Fig. 2. This shows that a new platform for optoelectronic innovation is on the way [71, 72].

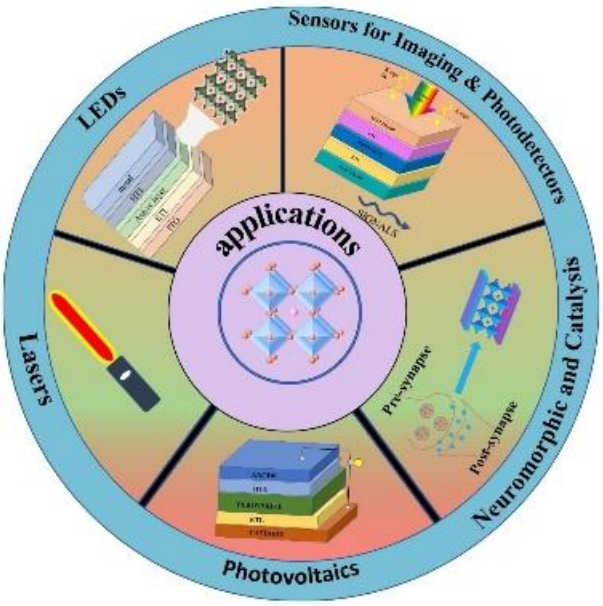

Fig. 2. Application of perovskite material.

Photovoltaics (Perovskite Solar Cells - PSCs): So far, the best use of perovskites has been in photovoltaics, where they have changed the way people perceive solution-processed solar cells. The standard device architecture has changed from a mesoporous scaffold to a planar heterojunction, which can be either an n-i-p or an inverted p-i-n configuration. This gives you greater flexibility for materials and manufacturing [73]. In just over ten years, the power conversion efficiency (PCE) of single-junction perovskite solar cells (PSCs) has gone from 3.8% to more than 26%. This is a growth rate that no other photovoltaic technology can match [74]. The ability to change the perovskite bandgap makes them preferable for tandem solar cells than single-junction cells. Perovskite/silicon tandem cells have certified efficiencies greater than 33%, which is much higher than the theoretical limit for single-junction silicon cells [75]. The top cell is made of perovskite and absorbs high-energy photons, while the bottom cell is made of silicon and captures lower-energy photons. All-perovskite tandem solar cells, which integrate a wide-bandgap top cell with a low-bandgap (~1.25 eV) tin-lead (Sn-Pb) bottom cell, have made big strides, reaching efficiencies over 28%. This shows that photovoltaics are moving toward being lightweight, flexible, and extremely effective [76], a simple illustration, "power generation" is given by Fig. 3.

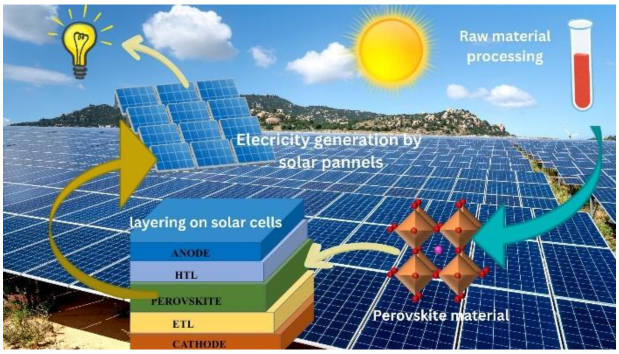

Fig. 3. Creation of power from perovskite based solar panels.

Phosphorescent Light-Emitting Diodes (PeLEDs): The characteristics that make perovskites great at absorbing light—high photoluminescence quantum yield (PLQY), narrow emission linewidth (high color purity), and facile bandgap tunability—also make them great at emitting light. Perovskite light-emitting diodes (PeLEDs) have made a lot of progress in just a brief span of time. Through meticulous defect passivation, dimensional regulation (including the use of quasi-2D perovskites for energy funneling), and cutting-edge device engineering, the external quantum efficiency (EQE) of green and red PeLEDs has surpassed 30%, approaching the theoretical maximum and directly competing with established organic LED (OLED) technologies [76, 77]. Achieving efficient and persistent blue emission is significantly challenging due to halide segregation and high defect concentrations in wider-bandgap materials. Still, PeLEDs are an excellent pick for future display and lighting applications since they have good color purity and can be made cheaply.

Sensors for Imaging and Photodetectors: Perovskites are among the most suitable semiconductors for photodetection because they have an elevated absorption coefficient, which makes it less difficult to make thin active layers, and because they have great charge transport properties, which makes them react quickly. By changing the halide composition, perovskite photodetectors can be made to work throughout a wide range of wavelengths, from ultraviolet to visible and near-infrared [78]. They display enhanced responsivity and detectivity, which are measures of how sensitive they are to light, compared with commercial photodetectors made of silicon or III-V compounds. Recent innovation has successfully integrated perovskite photodetector arrays into high-resolution image sensors for visible-light and X-ray imaging, which led to a combination of high sensitivity, low dose requirements, and potential cost advantages over existing technologies [79].

Lasers: Perovskite materials are outstanding options for optical amplification and lasing because they have very few defects that cause non-radiative recombination and high gain coefficients. Perovskites have demonstrated lasing over the visible spectrum using optical pumping in various topologies, including whispering gallery mode resonators and distributed feedback (DFB) gratings, noted for their low lasing thresholds. The field is currently making progress toward the development of continuous-wave (CW) and electrically pumped lasers. Recent demonstrations of continuous-wave optically pumped lasing at room temperature represent a significant milestone towards the ultimate goal of a perovskite laser diode, enabling compact, tunable, and economical coherent light sources [80].

Newer Uses: The range of uses for perovskites is continually getting more. Because they have large atomic numbers (like Pb and I) and are good at transferring charge, they are great X-ray and gamma-ray detectors. They could be more reactive and have better resolution at a lower cost than current technologies like amorphous selenium. Companies are currently bringing perovskite-based X-ray imaging panels to market, taking use of these benefits [79].The ion migration mechanism in electronics, usually a drawback for solar cells, is used in memristors for neuromorphic computing, allowing perovskite devices to mimic cerebral plasticity [81]. Additionally, some perovskite compositions demonstrate promising catalytic effectiveness for processes like as photocatalytic CO_2 reduction and water splitting, despite this field still being in its early stages of research [80].

6. KEY CHALLENGES AND DEGRADATION MECHANISMS

The impressive performance gains are greatly limited by the fact that perovskite optoelectronics aren't very stable when they're in use, which makes them less commercially viable. The degradation of perovskite materials is a complex phenomenon involving intrinsic thermodynamic instabilities and external environmental factors, which often interact to accelerate device failure. A comprehensive understanding of these mechanisms is the preliminary phase in developing mitigation strategies [41, 42].

Stability in Operations and Intrinsic: Perovskite devices have a shorter operational lifespan because they are sensitive to several kinds of environmental and operational pressures. Moisture and oxygen are known to speed up decomposition. Water molecules can catalyze the reversible hydrolysis of organic cations and promote irreversible crystal phase transitions. Oxygen, on the other hand, can permeate the film and act as a trap state, which increases non-radiative recombination and photo-oxidation processes [82, 83]. Additionally, heat generated during prolonged operation or in outdoor environments can accelerate these chemical reactions, facilitate the volatilization of organic components, and trigger detrimental phase transitions from the photoactive phase to inactive states (e.g., the yellow δ-phase of $FAPbI_3$), markedly degrading performance [84].

Photo-induced degradation under operational settings, along with external variables, is a major obstacle. Light, especially UV radiation, can damage the charge transport layers and create reactive species that harm the perovskite layer. A more specific and significant issue is phase segregation under bias, often termed halide segregation. In mixed-halide perovskites (e.g., $MAPb(I_{1-x}Br_x)_3$), light and electrical bias can cause halides to separate into areas that are rich in iodine and areas that are rich in bromine. This segregation distorts the bandgap, creating low-bandgap pathways that trap charge carriers. This causes a red shift in photoluminescence and a drop in photovoltaic voltage [85]. Recent research has explicitly linked this behavior to the formation of polaronic states and lattice strain, providing a deeper mechanistic understanding that is guiding the development of novel suppression strategies [86].

The main problem that comes with this is ion migration. The flexible ionic lattice of perovskites makes it easy for both anions (I^-, Br^-) and cations (MA^+, Pb^{2+} vacancies) to move around when there is an electric field, even when the temperature is normal. This behavior immediately leads to the current-voltage (I-V) hysteresis that is often seen in solar cell measurements and is a key factor in long-term damage. It can cause metal electrodes (such Ag or Al) to corrode faster, break down the perovskite material faster, and create metastable phases and defect clusters that act as recombination centers [87, 88].

Environmental and Toxicity Problems: The presence of lead (Pb) in the highest-performing perovskite formulations poses the primary obstacle to public image and environmental sustainability. The amount of lead in each gadget is small, but it can dissolve in water, which makes it a big problem if the modules are broken or thrown away wrong after they are no longer needed [89]. There are many rules that limit how lead can be used, such as the EU's Restriction of Hazardous Substances (RoHS) Regulation. Therefore, addressing the "lead problem" is crucial for societal acceptance, regulatory compliance, and ethical commercialization [90, 91].

The main environmental risk comes from soluble Pb^{2+} ions leaking out of broken modules because of rain. Research suggests that lead can leach at concentrations exceeding legal drinking water standards, highlighting the inadequacy of present solar panel encapsulation for complete containment [91]. Life-cycle analysis (LCA) studies have been conducted to thoroughly evaluate the environmental impact. The studies show that the situation is more complicated than it seems. Even though making perovskite solar cells (PSCs) usually uses less energy and releases less greenhouse gases than making silicon photovoltaics, the possible environmental effects at the end of life, due to lead leakage, can have a big effect on the overall balance of the ecosystem [92]. The results of LCAs are greatly affected by how long devices last, how well they are contained, and how they are recycled. This shows that we need to make strong recycling programs and truly effective containment methods.

Scalability and Making: It is a big engineering problem to go from small, high-efficiency champion cells made in controlled circumstances to huge, commercially viable modules. Moving from lab-scale (<1 cm^2) to module-scale (>100 cm^2) makes it hard to learn how to control the kinetics of coating and crystallization on large surfaces. This includes controlling fluid dynamics, drying kinetics, and nucleation uniformity to avoid defects like pinholes and differences in thickness that seriously hurt performance. Moreover, manufacturing requires the sequential application of multiple layers, each with unique processing specifications, in conjunction with advanced laser scribing techniques to create monolithic interconnections, which may result in defects and reduce the active area [93, 94].

The issue of reproducibility and uniformity over large areas is strongly related. The crystallization of perovskite films is significantly affected by several factors, including precursor ink composition, ambient conditions (temperature and humidity), substrate wettability, and post-deposition treatment. Minor, unintentional deviations can result in significant variations in film morphology, crystallinity, and ultimately device performance, resulting in unacceptable "batch-to-batch" variability in industrial production [22, 95]. Achieving uniformity over a meter-sized substrate is quite difficult and requires advanced in-situ monitoring and real-time feedback management systems to efficiently control the coating environment.

7. STRATEGIES FOR IMPROVEMENT AND MITIGATION

The major problems facing perovskite optoelectronics have led to a wide spectrum of creative solutions. Research has evolved beyond merely pinpointing problems to developing complex, multi-faceted solutions that tackle degradation and inefficiency at the atomic, microstructural, device, and module levels. A complete plan that combines these strategies is now making gadgets that last longer and work better [96, 97].

Making Stability Better: The main defense is compositional engineering, which aims to stabilize the perovskite lattice. Adding mixed cations (like $FA^+/Cs^+/MA^+/Rb^+$) and mixed halides (like I^-/Br^-) helps keep volatile organic compounds from forming and stops detrimental phase changes, which improves thermal and phase stability [98]. Recent advancements employ volatile alkylammonium salts (e.g., phenethyl ammonium iodide) that vaporize during annealing, yielding a stabilized three-dimensional lattice with passivated defects. This technique has attained unparalleled operational stability for perovskite/silicon tandem devices [99]. Combining pseudohalides like thiocyanate (SCN^-) and formate ($HCOO^-$) is still one of the best ways to stop halide segregation and ion migration in wide-bandgap perovskites [100].

Additive engineering is a good way to fix problems at grain boundaries and surfaces. By coordinating with Pb^{2+} ions that aren't coordinated enough and filling in halide vacancies, molecular additives such polymers and fullerene derivatives help fix ionic defects in the precursor solution [101]. Recent developments focus on multi-functional additives that simultaneously passivate both anionic and cationic defects. Carbonyl and amine groups in molecules can effectively reduce I^- vacancies and Pb^+-related defects, leading to improvements in both efficiency and stability at the same time [102].

Interface and contact engineering are crucial, as interfaces often signify the critical point at which degradation initiates. The development of stable inorganic charge transport layers, such as NiO_x for hole transport layers and SnO_2 for electron transport layers, has replaced hygroscopic and unstable organic materials like spiro-OMeTAD [103]. Using ultra-thin passivating interlayers, like self-assembled monolayers (SAMs), between the perovskite and the charge transport layer can stop ions from moving and stop bad chemical processes [104]. In the end, advanced encapsulation methods provide an important layer of protection from the outside. Hermetic glass-glass encapsulation with strong edge sealing and built-in desiccants is very important for keeping moisture and oxygen from getting in. Engineers are working on multilayer barrier films with alternating organic and inorganic layers that can be used in a variety of ways to achieve the ultra-low water vapor transmission rates needed to meet commercial lifespan goals [21, 99].

Replacing Lead (Pb): The quest for possible lead-free replacements is a major area of research that focuses on many types of materials, each of which has its own pros and cons. Tin (Sn)-based perovskites are the most promising direct replacement because their electrical structure is similar. The main issue is that Sn^{2+} can easily turn into Sn^{4+}. Mitigation strategies have advanced significantly, employing robust reducing agents (e.g., Sn^0 powder) and functional antioxidants (e.g., gallic acid) that establish a more vigorous reducing environment within the film bulk and during operation, leading to improved efficiency and stability [105]. Double Perovskites, like $Cs_2AgBiBr_6$, are quite stable, yet they usually exhibit indirect bandgaps. Recent research has focused on alloying (e.g., Na alloying) and Nano structuring to alter the band structure and improve charge carrier mobility, hence enhancing efficiency [106]. Additional Options: Bismuth (Bi) and Antimony (Sb)-based perovskites (for example, $Cs_3Sb_2I_9$) are very stable but have big bandgaps. Researchers are looking into dimensions reduction (2D/3D hybrids) and defect engineering to improve their optoelectronic capabilities [107].

A significant theme among all lead-free perovskites is the notable compromise between performance and stability. The current method entails accepting a slight decrease in initial efficiency in exchange for a substantial increase in internal stability, a compromise that may be beneficial for some market applications.

Growth and Entry into the Market: Building strong procedures is a key part of scaling strategies. This means moving from spin-coating to larger deposition technologies like blade coating and slot-die coating. The main enabler is the development of ink formulations with a broad "processing window"—inks that can handle changes in coating speed, temperature, and environmental conditions—which is necessary for getting high repeatability on industrial production lines [108]. In situ monitoring tools that are cutting-edge, like optical coherence tomography and photoluminescence imaging, are now being added to pilot lines to give real-time feedback and control over the crystallization process. This will make sure that large areas stay consistent The International Summit on Organic Photovoltaic Stability (ISOS) is one example of an international stability testing protocol that is providing standardized metrics to accurately compare the longevity of devices from different research groups and companies. This is making people more confident in the technology's durability [93].

8. FUTURE PERSPECTIVE

To make perovskite photovoltaics commercially viable, we need to fix the problems with their stability and scalability. Researchers are working on making low-dimensional (2D/3D) heterostructures and molecular additives that passivate defects to make the materials more resistant to heat, light, and moisture in the environment and when they are in use [9, 109]. At the same time, scalable manufacturing processes like slot-die coating, inkjet printing, and vapor-phase deposition are being improved to make it easier to make homogeneous, large-area modules quickly while keeping high efficiency [19, 110]. Combining all-perovskite tandem structures with silicon or CIGS bottom cells is a good way to break the single-junction Shockley-Queisser limit and raise efficiencies to 30% or more [75, 111].Standardized stability testing methods, lead-free or sequestration technologies, and the creation of strong, flexible designs for building-integrated and portable power applications [112, 113] will all be important for the successful move from the lab to the market.

REFERENCES

[1] D. B. Mitzi, "Synthesis, structure, and properties of Organic-Inorganic Perovskites and related materials," *Progress in Inorganic Chemistry*, pp. 1–121, Jan. 1999, doi: 10.1002/9780470166499.ch1.

[2] D. Weber, "CH3NH3PbX3, ein Pb(II)-System mit kubischer Perowskitstruktur / CH3NH3PbX3, a Pb(II)-System with Cubic Perovskite Structure," *Zeitschrift Für Naturforschung B*, vol. 33, no. 12, pp. 1443–1445, Dec. 1978, doi: 10.1515/znb-1978-1214.

[3] D. B. Mitzi, C. A. Feild, W. T. A. Harrison, and A. M. Guloy, "Conducting tin halides with a layered organic-based perovskite structure," *Nature*, vol. 369, no. 6480, pp. 467–469, Jun. 1994, doi: 10.1038/369467a0.

[4] D. B. Mitzi, K. Chondroudis, and C. R. Kagan, "Organic-inorganic electronics," *IBM Journal of Research and Development*, vol. 45, no. 1, pp. 29–45, Jan. 2001, doi: 10.1147/rd.451.0029.

[5] A. Kojima, K. Teshima, Y. Shirai, and T. Miyasaka, "Organometal halide perovskites as Visible-Light sensitizers for photovoltaic cells," *Journal of the American Chemical Society*, vol. 131, no. 17, pp. 6050–6051, Apr. 2009, doi: 10.1021/ja809598r.

[6] H.-S. Kim *et al.*, "Lead Iodide Perovskite Sensitized All-Solid-State Submicron Thin Film Mesoscopic Solar Cell with Efficiency Exceeding 9%," *Scientific Reports*, vol. 2, no. 1, p. 591, Aug. 2012, doi: 10.1038/srep00591.

[7] M. M. Lee, J. Teuscher, T. Miyasaka, T. N. Murakami, and H. J. Snaith, "Efficient hybrid solar cells based on Meso-Superstructured organometal halide perovskites," *Science*, vol. 338, no. 6107, pp. 643–647, Oct. 2012, doi: 10.1126/science.1228604.

[8] M. S. Seveda, P. D. Narale, and S. N. Kharpude, *Advances in renewable energy engineering*. 2024.

[9] J. Jeong *et al.*, "Pseudo-halide anion engineering for α-FAPbI3 perovskite solar cells," *Nature*, vol. 592, no. 7854, pp. 381–385, Apr. 2021, doi: 10.1038/s41586-021-03406-5.

[10] M. Saliba *et al.*, "Cesium-containing triple cation perovskite solar cells: improved stability, reproducibility and high efficiency," *Energy & Environmental Science*, vol. 9, no. 6, pp. 1989–1997, Jan. 2016, doi: 10.1039/c5ee03874j.

[11] Z.-K. Tan *et al.*, "Bright light-emitting diodes based on organometal halide perovskite," *Nature Nanotechnology*, vol. 9, no. 9, pp. 687–692, Aug. 2014, doi: 10.1038/nnano.2014.149.

[12] B. R. Sutherland and E. H. Sargent, "Perovskite photonic sources," *Nature Photonics*, vol. 10, no. 5, pp. 295–302, Apr. 2016, doi: 10.1038/nphoton.2016.62.

[13] S. D. Stranks and H. J. Snaith, "Metal-halide perovskites for photovoltaic and light-emitting devices," *Nature Nanotechnology*, vol. 10, no. 5, pp. 391–402, May 2015, doi: 10.1038/nnano.2015.90.

[14] C. Wehrenfennig, G. E. Eperon, M. B. Johnston, H. J. Snaith, and L. M. Herz, "High charge carrier mobilities and lifetimes in organolead trihalide perovskites," *Advanced Materials*, vol. 26, no. 10, pp. 1584–1589, Dec. 2013, doi: 10.1002/adma.201305172.

[15] K. Wang, D. Yang, C. Wu, M. Sanghadasa, and S. Priya, "Recent progress in fundamental understanding of halide perovskite semiconductors," *Progress in Materials Science*, vol. 106, p. 100580, Jul. 2019, doi: 10.1016/j.pmatsci.2019.100580.

[16] S. P. Dunfield *et al.*, "From Defects to degradation: A mechanistic understanding of degradation in perovskite solar cell devices and modules," *Advanced Energy Materials*, vol. 10, no. 26, Mar. 2020, doi: 10.1002/aenm.201904054.

[17] F. Giustino and H. J. Snaith, “Toward Lead-Free Perovskite solar cells,” *ACS Energy Letters*, vol. 1, no. 6, pp. 1233–1240, Nov. 2016, doi: 10.1021/acsenergylett.6b00499.

[18] Z. Li *et al.*, “Scalable fabrication of perovskite solar cells,” *Nature Reviews Materials*, vol. 3, no. 4, Mar. 2018, doi: 10.1038/natrevmats.2018.17.

[19] N.-G. Park and K. Zhu, “Scalable fabrication and coating methods for perovskite solar cells and solar modules,” *Nat Rev Mater*, vol. 5, no. 5, pp. 333–350, Feb. 2020, doi: 10.1038/s41578-019-0176-2.

[20] M. Saliba, J. Correa-Baena, M. Grätzel, A. Hagfeldt, and A. Abate, “Perovskite solar cells: from the atomic level to film quality and device performance,” *Angewandte Chemie International Edition*, vol. 57, no. 10, pp. 2554–2569, May 2017, doi: 10.1002/anie.201703226.

[21] R. Cheacharoen *et al.*, “Encapsulating perovskite solar cells to withstand damp heat and thermal cycling,” *Sustainable Energy & Fuels*, vol. 2, no. 11, pp. 2398–2406, Jan. 2018, doi: 10.1039/c8se00250a.

[22] Y. Rong *et al.*, “Challenges for commercializing perovskite solar cells,” *Science*, vol. 361, no. 6408, Sep. 2018, doi: 10.1126/science.aat8235.

[23] B. Saparov and D. B. Mitzi, “Organic–Inorganic perovskites: structural versatility for functional materials design,” *Chemical Reviews*, vol. 116, no. 7, pp. 4558–4596, Apr. 2016, doi: 10.1021/acs.chemrev.5b00715.

[24] V. M. Goldschmidt, “Die Gesetze der Krystallochemie,” *Die Naturwissenschaften*, vol. 14, no. 21, pp. 477–485, May 1926, doi: 10.1007/bf01507527.

[25] C. Li, X. Lu, W. Ding, L. Feng, Y. Gao, and Z. Guo, “Formability of ABX 3 (X = F, Cl, Br, I) halide perovskites,” *Acta Crystallographica Section B Structural Science*, vol. 64, no. 6, pp. 702–707, Nov. 2008, doi: 10.1107/s0108768108032734.

[26] M. T. Weller, O. J. Weber, J. M. Frost, and A. Walsh, “Cubic Perovskite Structure of Black Formamidinium Lead Iodide, α-[HC(NH2)2]PbI3, at 298 K,” *The Journal of Physical Chemistry Letters*, vol. 6, no. 16, pp. 3209–3212, Aug. 2015, doi: 10.1021/acs.jpclett.5b01432

[27] S. Lu, Q. Zhou, Y. Ouyang, Y. Guo, Q. Li, and J. Wang, “Accelerated discovery of stable lead-free hybrid organic-inorganic perovskites via machine learning,” *Nature Communications*, vol. 9, no. 1, p. 3405, Aug. 2018, doi: 10.1038/s41467-018-05761-w.

[28] M. Qin *et al.*, “Regulating the Crystallization Kinetics and Lattice Strain of Lead-Free Perovskites with Perovskite Quantum Dots,” *ACS Energy Letters*, vol. 7, no. 10, pp. 3251–3259, Sep. 2022, doi: 10.1021/acsenergylett.2c01692.

[29] B. V. Stefani *et al.*, “Historical market projections and the future of silicon solar cells,” *Joule*, vol. 7, no. 12, pp. 2684–2699, Dec. 2023, doi: 10.1016/j.joule.2023.11.006.

[30] N. Zheng *et al.*, “Synthesis of zero-dimensional octahedral metal halides through solvent incorporation and their photophysical properties,” *Nature Chemistry*, vol. 17, no. 9, pp. 1401–1409, Aug. 2025, doi: 10.1038/s41557-025-01869-x.

[31] J. H. Noh, S. H. Im, J. H. Heo, T. N. Mandal, and S. I. Seok, “Chemical management for colorful, efficient, and stable Inorganic–Organic Hybrid nanostructured solar cells,” *Nano Letters*, vol. 13, no. 4, pp. 1764–1769, Mar. 2013, doi: 10.1021/nl400349b.

[32] H. Tsai *et al.*, “High-efficiency two-dimensional Ruddlesden–Popper perovskite solar cells,” *Nature*, vol. 536, no. 7616, pp. 312–316, Jul. 2016, doi: 10.1038/nature18306.

[33] L. Mao, C. C. Stoumpos, and M. G. Kanatzidis, “Two-Dimensional Hybrid Halide Perovskites: Principles and promises,” *Journal of the American Chemical Society*, vol. 141, no. 3, pp. 1171–1190, Nov. 2018, doi: 10.1021/jacs.8b10851.

[34] J. Qing *et al.*, “Spacer cation engineering in Ruddlesden-Popper perovskites for efficient red light-emitting diodes with recommendation 2020 color coordinates,” *Applied Surface Science*, vol. 616, p. 156454, Jan. 2023, doi: 10.1016/j.apsusc.2023.156454.

[35] C. Zhou *et al.*, “Luminescent zero-dimensional organic metal halide hybrids with near-unity quantum efficiency,” *Chemical Science*, vol. 9, no. 3, pp. 586–593, Nov. 2017, doi: 10.1039/c7sc04539e.

[36] B. Li, Y. Xu, X. Zhang, K. Han, J. Jin, and Z. Xia, “Zero-Dimensional luminescent metal halide hybrids enabling bulk transparent medium as Large-Area X-Ray scintillators,” *Advanced Optical Materials*, vol. 10, no. 10, Mar. 2022, doi: 10.1002/adom.202102793.

[37] C. C. Stoumpos, C. D. Malliakas, and M. G. Kanatzidis, “Semiconducting Tin and Lead Iodide Perovskites with Organic Cations: Phase Transitions, High Mobilities, and Near-Infrared Photoluminescent Properties,” *Inorganic Chemistry*, vol. 52, no. 15, pp. 9019–9038, Jul. 2013, doi: 10.1021/ic401215x.

[38] S. Mariotti *et al.*, "Interface engineering for high-performance, triple-halide perovskite–silicon tandem solar cells," *Science*, vol. 381, no. 6653, pp. 63–69, Jul. 2023, doi: 10.1126/science.adf5872.

[39] R. Lin *et al.*, "All-perovskite tandem solar cells with 3D/3D bilayer perovskite heterojunction," *Nature*, vol. 620, no. 7976, pp. 994–1000, Jun. 2023, doi: 10.1038/s41586-023-06278-z.

[40] S. De Wolf *et al.*, "Organometallic halide perovskites: sharp optical absorption edge and its relation to photovoltaic performance," *The Journal of Physical Chemistry Letters*, vol. 5, no. 6, pp. 1035–1039, Mar. 2014, doi: 10.1021/jz500279b.

[41] R. K. Miao *et al.*, "Electroosmotic flow steers neutral products and enables concentrated ethanol electroproduction from CO2," *Joule*, vol. 5, no. 10, pp. 2742–2753, Sep. 2021, doi: 10.1016/j.joule.2021.08.013.

[42] C. Wang, "Unlocking the potential of ultrahigh-Ni cathodes via epitaxial entropy-assisted coating," *Nature Reviews Materials*, vol. 9, no. 5, p. 303, Apr. 2024, doi: 10.1038/s41578-024-00686-x.

[43] D. Mondal, M. Ahmad, B. Dey, A. Mondal, and P. Talukdar, "Formation of supramolecular channels by reversible unwinding-rewinding of bis(indole) double helix via ion coordination," *Nature Communications*, vol. 13, no. 1, p. 6507, Oct. 2022, doi: 10.1038/s41467-022-34159-y.

[44] H. Wang, L. Valkunas, T. Cao, L. Whittaker-Brooks, and G. R. Fleming, "Coulomb screening and coherent phonon in methylammonium lead iodide perovskites," *The Journal of Physical Chemistry Letters*, vol. 7, no. 16, pp. 3284–3289, Aug. 2016, doi: 10.1021/acs.jpclett.6b01425.

[45] S. D. Stranks *et al.*, "Electron-Hole diffusion lengths exceeding 1 micrometer in an organometal trihalide perovskite absorber," *Science*, vol. 342, no. 6156, pp. 341–344, Oct. 2013, doi: 10.1126/science.1243982.

[46] Q. Jiang *et al.*, "Surface passivation of perovskite film for efficient solar cells," *Nature Photonics*, vol. 13, no. 7, pp. 460–466, Apr. 2019, doi: 10.1038/s41566-019-0398-2.

[47] R. Lin *et al.*, "All-perovskite tandem solar cells with improved grain surface passivation," *Nature*, vol. 603, no. 7899, pp. 73–78, Jan. 2022, doi: 10.1038/s41586-021-04372-8.

[48] A. Miyata *et al.*, "Direct measurement of the exciton binding energy and effective masses for charge carriers in organic–inorganic tri-halide perovskites," *Nature Physics*, vol. 11, no. 7, pp. 582–587, Jun. 2015, doi: 10.1038/nphys3357.

[49] Q. Jiang and K. Zhu, "Rapid advances enabling high-performance inverted perovskite solar cells," *Nature Reviews Materials*, vol. 9, no. 6, pp. 399–419, May 2024, doi: 10.1038/s41578-024-00678-x.

[50] C. Zhang, "Breaking free from high pressure," *Nature Energy*, vol. 9, no. 2, p. 109, Feb. 2024, doi: 10.1038/s41560-024-01477-y.

[51] A. Ecija, K. Vidal, A. Larraaga, L. Ortega-San-Martn, and M. Isabel, "Synthetic methods for perovskite Materials; structure and morphology," in *InTech eBooks*, 2012. doi: 10.5772/36540.

[52] D. Kumar, R. S. Yadav, Monika, A. K. Singh, and S. B. Rai, "Synthesis techniques and applications of perovskite materials," in *IntechOpen eBooks*, 2020. doi: 10.5772/intechopen.86794.

[53] S. I. Terhemba *et al.*, "Review on green Methods of photocatalytic degradation using nascent perovskites," *African Journal of Pure and Applied Sciences*, vol. 6, no. 1, pp. 46–57, Jun. 2025, doi: 10.33886/ajpas.v6i1.649.

[54] S. A. Kulkarni, S. G. Mhaisalkar, N. Mathews, and P. P. Boix, "Perovskite nanoparticles: synthesis, properties, and novel applications in photovoltaics and LEDs," *Small Methods*, vol. 3, no. 1, Oct. 2018, doi: 10.1002/smtd.201800231.

[55] M. Singh, B. C. Yadav, A. Ranjan, M. Kaur, and S. K. Gupta, "Synthesis and characterization of perovskite barium titanate thin film and its application as LPG sensor," *Sensors and Actuators B Chemical*, vol. 241, pp. 1170–1178, Oct. 2016, doi: 10.1016/j.snb.2016.10.018.

[56] X. Liu, L. Cao, Z. Guo, Y. Li, W. Gao, and L. Zhou, "A review of perovskite photovoltaic materials' synthesis and applications via chemical vapor deposition method," *Materials*, vol. 12, no. 20, p. 3304, Oct. 2019, doi: 10.3390/ma12203304.

[57] X. Lu, X. Fan, H. Zhang, Q. Xu, and M. Ijaz, "Review on preparation of perovskite solar cells by Pulsed Laser Deposition," *Inorganics*, vol. 12, no. 5, p. 128, Apr. 2024, doi: 10.3390/inorganics12050128.

[58] Z. Long *et al.*, "All-inorganic halide perovskite (CsPbX3, X=Cl, Br, I) quantum dots synthesized via fast anion hot injection by using trimethylhalosilanes," *Ceramics International*, vol. 48, no. 23, pp. 35474–35479, Aug. 2022, doi: 10.1016/j.ceramint.2022.08.153.

[59] S. Zang, J. Chen, Y. Yu, X. Qin, and H. Liu, "Ligand-Assisted reprecipitation of highly luminescent perovskite nanocrystals," *ACS Applied Nano Materials*, vol. 8, no. 7, pp. 3680–3687, Feb. 2025, doi: 10.1021/acsanm.5c00412.

[60] A. Pramanik, S. Patibandla, Y. Gao, K. Gates, and P. C. Ray, "Water triggered synthesis of highly stable and biocompatible 1D nanowire, 2D nanoplatelet, and 3D nanocube CSPBBR3 perovskites for multicolor Two-Photon cell imaging," *JACS Au*, vol. 1, no. 1, pp. 53–65, Dec. 2020, doi: 10.1021/jacsau.0c00038.

[61] D. Zhang *et al.*, "Metal Halide Perovskite nanowires: Synthesis, integration, Properties, and Applications in Optoelectronics," *Advanced Energy Materials*, vol. 13, no. 33, Aug. 2022, doi: 10.1002/aenm.202201735.

[62] Z. Yuan *et al.*, "Growing MASnI3 perovskite single-crystal films by inverse temperature crystallization," *Journal of Physics Condensed Matter*, vol. 34, no. 14, p. 144009, Jan. 2022, doi: 10.1088/1361-648x/ac4c64.

[63] N. Grundmanis, A. Sarakovskis, A. Lupilov, V. Gostilo, A. Owens, and K. Pudzs, "The X- and gamma-ray detection properties of CsPbBr3 perovskite crystals grown by the Bridgman–Stockbarger method," *Nuclear Instruments and Methods in Physics Research Section a Accelerators Spectrometers Detectors and Associated Equipment*, vol. 1073, p. 170305, Feb. 2025, doi: 10.1016/j.nima.2025.170305.

[64] J. Sun, F. Li, J. Yuan, and W. Ma, "Advances in Metal halide Perovskite Film Preparation: The role of Anti-Solvent Treatment," *Small Methods*, vol. 5, no. 5, p. e2100046, Feb. 2021, doi: 10.1002/smtd.202100046.

[65] H.-C. Cha, S.-H. Huang, C.-F. Li, F.-Y. Tsai, W.-F. Su, and Y.-C. Huang, "Advances and strategies in scalable coating techniques for flexible perovskite solar cells," *Sustainable Energy & Fuels*, vol. 9, no. 22, pp. 5962–6006, Jan. 2025, doi: 10.1039/d5se00873e.

[66] A. Paliwal, K. P. S. Zanoni, C. Roldán-Carmona, M. A. Hernández-Fenollosa, and H. J. Bolink, "Fully vacuum-deposited perovskite solar cells in substrate configuration," *Matter*, vol. 6, no. 10, pp. 3499–3508, Aug. 2023, doi: 10.1016/j.matt.2023.07.011.

[67] U. Saeed, F. Sandiumenge, K. Cordero-Edwards, J. Padilla-Pantoja, J. M. Caicedo Roque, D. Pesquera, J. Santiso, and G. Catalan, "Pervasive protonation of perovskite membranes made by the water-soluble sacrificial layer method," *arXiv preprint arXiv:2503.04197*, 2025.

[68] Y. Kim *et al.*, "Remote epitaxy through graphene enables two-dimensional material-based layer transfer," *Nature*, vol. 544, no. 7650, pp. 340–343, Apr. 2017, doi: 10.1038/nature22053.

[69] X. Peng *et al.*, "Perovskite and organic solar cells fabricated by Inkjet Printing: progress and prospects," *Advanced Functional Materials*, vol. 27, no. 41, Sep. 2017, doi: 10.1002/adfm.201703704.

[70] B. Jeong, H. Han, H. H. Kim, W. K. Choi, Y. J. Park, and C. Park, "Polymer-Assisted nanoimprinting for Environment- and Phase-Stable perovskite nanopatterns," *ACS Nano*, vol. 14, no. 2, pp. 1645–1655, Jan. 2020, doi: 10.1021/acsnano.9b06980.

[71] N. Kinsey, C. DeVault, A. Boltasseva, and V. M. Shalaev, "Near-zero-index materials for photonics," *Nature Reviews Materials*, vol. 4, no. 12, pp. 742–760, Sep. 2019, doi: 10.1038/s41578-019-0133-0.

[72] X. Huang, T. Li, W. Fan, R. Xiao, and X. Cheng, "Challenges and Solutions of Solid-State Electrolyte Film for Large-Scale Applications," *Advanced Energy Materials*, vol. 14, no. 11, Jan. 2024, doi: 10.1002/aenm.202303850.

[73] N. J. Jeon *et al.*, "Compositional engineering of perovskite materials for high-performance solar cells," *Nature*, vol. 517, no. 7535, pp. 476–480, Jan. 2015, doi: 10.1038/nature14133.

[74] J. J. Cordell, M. Woodhouse, and E. L. Warren, "Technoeconomic analysis of perovskite/silicon tandem solar modules," *Joule*, vol. 9, no. 2, p. 101781, Nov. 2024, doi: 10.1016/j.joule.2024.10.013.

[75] A. Al-Ashouri *et al.*, "Monolithic perovskite/silicon tandem solar cell with >29% efficiency by enhanced hole extraction," *Science*, vol. 370, no. 6522, pp. 1300–1309, Dec. 2020, doi: 10.1126/science.abd4016.

[76] K. Lin *et al.*, "Perovskite light-emitting diodes with external quantum efficiency exceeding 20 per cent," *Nature*, vol. 562, no. 7726, pp. 245–248, Oct. 2018, doi: 10.1038/s41586-018-0575-3.

[77] J. S. Kim *et al.*, "Ultra-bright, efficient and stable perovskite light-emitting diodes," *Nature*, vol. 611, no. 7937, pp. 688–694, Nov. 2022, doi: 10.1038/s41586-022-05304-w.

[78] F. P. G. De Arquer, A. Armin, P. Meredith, and E. H. Sargent, "Solution-processed semiconductors for next-generation photodetectors," *Nature Reviews Materials*, vol. 2, no. 3, Jan. 2017, doi: 10.1038/natrevmats.2016.100.

[79] H. Wei *et al.*, "Sensitive X-ray detectors made of methylammonium lead tribromide perovskite single crystals," *Nature Photonics*, vol. 10, no. 5, pp. 333–339, Mar. 2016, doi: 10.1038/nphoton.2016.41.

[80] L. Zhang *et al.*, "Advances in the application of perovskite materials," *Nano-Micro Letters*, vol. 15, no. 1, p. 177, Jul. 2023, doi: 10.1007/s40820-023-01140-3.

[81] R. A. John *et al.*, "Flexible Ionic-Electronic Hybrid Oxide Synaptic TFTs with Programmable Dynamic Plasticity for Brain-Inspired Neuromorphic Computing," *Small*, vol. 13, no. 32, Jun. 2017, doi: 10.1002/smll.201701193.

[82] G. Niu, X. Guo, and L. Wang, "Review of recent progress in chemical stability of perovskite solar cells," *Journal of Materials Chemistry A*, vol. 3, no. 17, pp. 8970–8980, Dec. 2014, doi: 10.1039/c4ta04994b.

[83] N. Aristidou *et al.*, "Fast oxygen diffusion and iodide defects mediate oxygen-induced degradation of perovskite solar cells," *Nature Communications*, vol. 8, no. 1, p. 15218, May 2017, doi: 10.1038/ncomms15218.

[84] B. Boro, S. Mishra, P. Singh, B. Lahiri, S. K. Varshney, and T. Singh, "Thermal Stability Analysis of Formamidinium–Cesium-Based Lead Halide Perovskite Solar Cells Fabricated under Air Ambient Conditions," *Energy Technology*, vol. 12, no. 8, May 2024, doi: 10.1002/ente.202400034.

[85] E. T. Hoke, D. J. Slotcavage, E. R. Dohner, A. R. Bowring, H. I. Karunadasa, and M. D. McGehee, "Reversible photo-induced trap formation in mixed-halide hybrid perovskites for photovoltaics," *Chemical Science*, vol. 6, no. 1, pp. 613–617, Nov. 2014, doi: 10.1039/c4sc03141e.

[86] L. Tian, J. Xue, and R. Wang, "Halide segregation in mixed halide perovskites: visualization and mechanisms," *Electronics*, vol. 11, no. 5, p. 700, Feb. 2022, doi: 10.3390/electronics11050700.

[87] A. Senocrate *et al.*, "The nature of ion conduction in methylammonium lead iodide: A multimethod approach," *Angewandte Chemie International Edition*, vol. 56, no. 27, pp. 7755–7759, May 2017, doi: 10.1002/anie.201701724.

[88] K. T. Tanko *et al.*, "The roles of ion migration on perovskite solar cell operational stability at various illumination intensities," *Solar RRL*, vol. 9, no. 12, Jun. 2025, doi: 10.1002/solr.202500162.

[89] A. Babayigit, A. Ethirajan, M. Muller, and B. Conings, "Toxicity of organometal halide perovskite solar cells," *Nature Materials*, vol. 15, no. 3, pp. 247–251, Feb. 2016, doi: 10.1038/nmat4572.

[90] A. D'Souza, H. Jones, and S. Gonthier, "Configuration management as a driver for sustainability," *INCOSE International Symposium*, vol. 35, no. 1, pp. 1166–1182, Jul. 2025, doi: 10.1002/iis2.70068.

[91] J. Li *et al.*, "Biological impact of lead from halide perovskites reveals the risk of introducing a safe threshold," *Nature Communications*, vol. 11, no. 1, p. 310, Jan. 2020, doi: 10.1038/s41467-019-13910-y.

[92] P. Sandwell *et al.*, "Off-grid solar photovoltaic systems for rural electrification and emissions mitigation in India," *Solar Energy Materials and Solar Cells*, vol. 156, pp. 147–156, May 2016, doi: 10.1016/j.solmat.2016.04.030.

[93] F. Deng, X. Song, Y. Li, W. Zhang, and X. Tao, "Facile eco-friendly process for upcycled sustainable perovskite solar cells," *Chemical Engineering Journal*, vol. 489, p. 151228, Apr. 2024, doi: 10.1016/j.cej.2024.151228.

[94] W. Tianhao *et al.*, "The main progress of perovskite solar cells in 2020–2021," *Institutional Repositories DataBase (IRDB)*, vol. 13, no. 152, Jul. 2021.

[95] W. Zhang *et al.*, "Strategies for improving efficiency and stability of inverted perovskite solar cells," *Advanced Materials*, vol. 36, no. 37, p. e2311025, Mar. 2024, doi: 10.1002/adma.202311025.

[96] P. Zhu *et al.*, "Aqueous synthesis of perovskite precursors for highly efficient perovskite solar cells," *Science*, vol. 383, no. 6682, pp. 524–531, Feb. 2024, doi: 10.1126/science.adj7081.

[97] D. Pyun *et al.*, "Machine Learning-Assisted prediction of Ambient-Processed perovskite solar cells' performances," *Energies*, vol. 17, no. 23, p. 5998, Nov. 2024, doi: 10.3390/en17235998.

[98] M. Saliba *et al.*, "A molecularly engineered hole-transporting material for efficient perovskite solar cells," *Nature Energy*, vol. 1, no. 2, Jan. 2016, doi: 10.1038/nenergy.2015.17.

[99] Q. Zhou *et al.*, "Annual research review of perovskite solar cells in 2023," *Materials Futures*, vol. 3, no. 2, p. 022102, Apr. 2024, doi: 10.1088/2752-5724/ad42ba.

[100] Y.-H. Lin *et al.*, "Bandgap-universal passivation enables stable perovskite solar cells with low photovoltage loss," *Science*, vol. 384, no. 6697, pp. 767–775, May 2024, doi: 10.1126/science.ado2302.

[101] X. Zheng *et al.*, "Defect passivation in hybrid perovskite solar cells using quaternary ammonium halide anions and cations," *Nature Energy*, vol. 2, no. 7, Jun. 2017, doi: 10.1038/nenergy.2017.102.

[102] C. Zhao *et al.*, "Stabilization of highly efficient perovskite solar cells with a tailored supramolecular interface," *Nature Communications*, vol. 15, no. 1, p. 7139, Aug. 2024, doi: 10.1038/s41467-024-51550-z.

[103] T. Bu *et al.*, "Surface modification via self-assembling large cations for improved performance and modulated hysteresis of perovskite solar cells," *Journal of Materials Chemistry A*, vol. 7, no. 12, pp. 6793–6800, Jan. 2019, doi: 10.1039/c8ta12284a.

[104] S. Tan *et al.*, "Sustainable thermal regulation improves stability and efficiency in all-perovskite tandem solar cells," *Nature Communications*, vol. 15, no. 1, p. 4136, May 2024, doi: 10.1038/s41467-024-48552-2.

[105] S. Jiang *et al.*, "Doping strategies for inorganic lead-free halide perovskite solar cells: progress and challenges," *Physical Chemistry Chemical Physics*, vol. 26, no. 6, pp. 4794–4811, Jan. 2024, doi: 10.1039/d3cp05444f.

[106] S. N. Rahane *et al.*, "Lead-Free Cs2AgBiCl6 Double Perovskite: Experimental and Theoretical Insights into the Self-Trapping for Optoelectronic Applications," *ACS Physical Chemistry Au*, vol. 4, no. 5, pp. 476–489, Jul. 2024, doi: 10.1021/acsphyschemau.4c00008.

[107] S. Rana and M. Akteruzzaman, "A comprehensive systematic literature review on perovskite solar cells: advancements, efficiency optimization, and commercialization Potential for Next-Generation photovoltaics," *SSRN Electronic Journal*, Jan. 2025, doi: 10.2139/ssrn.5237693.

[108] K. Zhuang *et al.*, "Multidimensional additive manufacturing for perovskite optoelectronic devices," *Advanced Materials*, vol. 38, no. 3, p. e14734, Oct. 2025, doi: 10.1002/adma.202514734.

[109] G. Grancini *et al.*, "One-Year stable perovskite solar cells by 2D/3D interface engineering," *Nature Communications*, vol. 8, no. 1, p. 15684, Jun. 2017, doi: 10.1038/ncomms15684.

[110] J. Feng *et al.*, "High-throughput large-area vacuum deposition for high-performance formamidine-based perovskite solar cells," *Energy & Environmental Science*, vol. 14, no. 5, pp. 3035–3043, Jan. 2021, doi: 10.1039/d1ee00634g.

[111] L. Li *et al.*, "Flexible all-perovskite tandem solar cells approaching 25% efficiency with molecule-bridged hole-selective contact," *Nature Energy*, vol. 7, no. 8, pp. 708–717, Jun. 2022, doi: 10.1038/s41560-022-01045-2.

[112] M. V. Khenkin *et al.*, "Consensus statement for stability assessment and reporting for perovskite photovoltaics based on ISOS procedures," *Nature Energy*, vol. 5, no. 1, pp. 35–49, Jan. 2020, doi: 10.1038/s41560-019-0529-5.

[113] H. Chen, L. Chu, and W. Yan, "Stability challenges in industrialization of perovskite photovoltaics: From Atomic-Scale view to module encapsulation," *Advanced Functional Materials*, vol. 35, no. 2, Oct. 2024, doi: 10.1002/adfm.202412389.